Depletion of oxygen, nitrate and nitrite in the Peruvian oxygen minimum zone cause an imbalance of benthic nitrogen fluxes

S. Sommer, J. Gier, T. Treude, U. Lomnitz, M. Dengler, J. Cardich, A.W. Dale

PII: S0967-0637(15)30081-9
DOI: http://dx.doi.org/10.1016/j.dsr.2016.03.001
Reference: DSRI2603

To appear in: *Deep-Sea Research Part I*

Received date: 6 August 2015
Revised date: 2 March 2016
Accepted date: 5 March 2016

Cite this article as: S. Sommer, J. Gier, T. Treude, U. Lomnitz, M. Dengler, J. Cardich and A.W. Dale, Depletion of oxygen, nitrate and nitrite in the Peruvian oxygen minimum zone cause an imbalance of benthic nitrogen fluxes, *Deep-Sea Research Part I,* http://dx.doi.org/10.1016/j.dsr.2016.03.001

Depletion of oxygen, nitrate and nitrite in the Peruvian oxygen minimum zone cause an imbalance of benthic nitrogen fluxes

Sommer S.[1]*, J. Gier.[1], T. Treude.[2], U. Lomnitz[1], M. Dengler [1], J. Cardich [3], A. W. Dale [1]

[1] GEOMAR Helmholtz Centre for Ocean Research Kiel, Wischhofstrasse 1-3, 24148 Kiel, Germany

[2] Department of Earth, Planetary & Space Science and Atmospheric and Oceanic Sciences, University of California, 595 Charles E. Young Drive East, Los Angeles, CA 90095, USA

[3] Department of Geochemistry, Universidade Federal Fluminense, Niterói, Rio de Janeiro, 24020-150, Brazil

* Corresponding author: Stefan Sommer, GEOMAR Helmholtz Centre for Ocean Research Kiel, Wischhofstrasse 1–3, 24148 Kiel, Germany, e–mail: ssommer@geomar.de

Abstract

Oxygen minimum zones (OMZ) are key regions for fixed nitrogen loss in both the sediments and the water column. During this study, the benthic contribution to N cycling was investigated at ten sites along a depth transect (74 – 989 m) across the Peruvian OMZ at 12°S. O_2 levels were below detection limit down to ~ 500 m. Benthic fluxes of N_2, NO_3^-, NO_2^-, NH_4^+, H_2S and O_2 were measured using benthic landers. Flux measurements on the shelf were made under extreme geochemical conditions consisting of a lack of O_2, NO_3^- and NO_2^- in the bottom water and elevated seafloor sulphide release. These particular conditions were associated with a large imbalance in the benthic nitrogen cycle. The sediments on the shelf were densely covered by filamentous sulphur bacteria *Thioploca*, and were identified as major recycling sites for DIN releasing high amounts of NH_4^+ up to 21.2 mmol m^{-2} d^{-1} that were far in excess of NH_4^+ release by ammonification. This difference was attributed to dissimilatory nitrate (or nitrite) reduction to ammonium (DNRA) that was partly being sustained by NO_3^- stored within the sulphur oxidizing bacteria. Sediments within the core of the OMZ (ca. 200 to 400 m) also displayed an excess flux of N of 3.5 mmol m^{-2} d^{-1} mainly as N_2. Benthic nitrogen and sulphur cycling in the Peruvian OMZ appears to be particularly susceptible to bottom water fluctuations in O_2, NO_3^- and NO_2^-, and may accelerate the onset of pelagic euxinia when NO_3^- and NO_2^- become depleted.

1. Introduction

A globally significant proportion of fixed nitrogen (N) loss proceeds in the relatively restricted marine areas known as ocean oxygen minimum zones (OMZ) due to the redox–sensitivity of N cycling processes (Gruber, 2004). Quantitative knowledge of the balance between fixed N source, sink and recycling pathways is required to understand feedbacks between surface water primary productivity and the maintenance or even spreading of OMZs (Stramma et al., 2008). N source/sink processes in the sediments form an integral part of the ecological status of OMZs, and of the oceans in general (Kalvelage et al., 2013; Devol, 2015).

The first in situ N flux measurements in the most productive upwelling system in the world off Peru (Bohlen et al., 2011) challenged the common understanding that shelf and slope sediments in high–nitrate–low–oxygen environments are mainly sinks for nitrate (NO_3^-) and nitrite (NO_2^-) by heterotrophic denitrification (Berelson et al., 1987; Devol and Christensen, 1993; Middelburg et al., 1996; Hartnett and Devol, 2003; Woulds et al., 2009). By combining flux measurements with pore water modelling, Bohlen et al. (2011) identified the anoxic Peruvian shelf and upper slope sediments at 11°S as important recycling sites for dissolved inorganic nitrogen (DIN, defined as $NO_3^- + NO_2^- + NH_4^+$ (ammonium)). A major proportion of the total $NO_3^- + NO_2^-$ uptake was channelled into dissimilatory nitrate reduction to ammonium (DNRA), producing NH_4^+ as an end product rather than N_2. DNRA contributed up to 80 % to the total benthic NH_4^+ release, with the remainder from organic nitrogen degradation (ammonification). In contrast to denitrification and anammox, DNRA retains DIN in the ecosystem, thereby opposing the self-cleansing effect of N loss via denitrification or anammox (Zopfi et al. 2001). The NH_4^+ released from the seabed is hypothesized to strongly contribute to pelagic anammox (Lam et al. 2009, Kalvelage et al. 2013) and, possibly, phototrophic primary production.

DNRA in Peruvian sediments is carried out by filamentous and nitrate-storing sulphur oxidizing chemolithotrophs belonging to the genera *Beggiatoa* and *Thioploca* (Jorgensen and Nelson, 2004). Reduction of NO_3^- and NO_2^- to NH_4^+ is accompanied by oxidation of dissolved sulfide (H_2S) to sulphate (SO_4^{2-}) via elemental sulphur as a reactive intermediate. DNRA performed by these and other sulphur bacteria is a globally widespread process (Jørgensen and Nelson, 2004; and references therein). Massive occurrence of these organisms has not only been reported from the Peruvian and Chilean continental shelf (e.g. Gallardo, 1977; Gutiérrez et al., 2008, Mosch et al. 2012, this study), but also from OMZ sediments of the Arabian Sea (Jørgensen and Gallardo, 1999; Schmaljohann et al., 2001) the Benguela current ecosystem off Namibia (Gallardo et al., 1998) and hypoxic environments in the Baltic Sea (Dale et al., 2013; Noffke et al., 2016). Communities of *Thioploca* on the Californian margin have been suspected to enhance N loss by shunting, either actively or passively, part of their internal NO_3^- reservoir to closely associated anammox bacteria (Prokopenko et al., 2013).

Dense mat communities of sulphur oxidising bacteria can significantly reduce the sulphide flux from the sediments to the overlying water column (Brüchert et al., 2003; Fossing et al., 1995; Teske, 2010, Teske and Nelson, 2006 and references therein; Zopfi et al., 2001). In organic carbon rich sediments with high rates of microbial sulphate reduction and underlying oxygen-depleted bottom waters, DNRA is an important sulfide detoxifying mechanism and gate-keeper between the benthic and pelagic sulphur and nitrogen cycle.

Members of the genus *Thioploca* very efficiently oxidize sulphide to levels near detection limit (Ferdelman et al., 1997; Thamdrup and Canfield, 1996; Bohlen et al., 2011). However, under sustained lack of bottom water oxygen (O_2), NO_3^- and NO_2^-, microbial sulphide production can overwhelm the sulphide oxidation capacity of the sulphur bacteria and lead to sulphide poisoning of life in the seabed (Gutiérrez et al., 2008). Sulphide-blackened dead

Thioploca mats referred to as "*Thioploca nigra*" have been frequently observed on Chilean shelf sediments (Teske, 2010)

Here we report on the benthic N fluxes across the Peruvian margin under conditions of high sulphide release from the shelf sediments and bottom waters that were depleted in NO_3^- and NO_2^-. At the time of sampling, the benthic N cycle at the shallowest stations was strongly shifted to a non-steady state regime. However, an imbalanced benthic N cycle was a general feature found down to 400 m, although not as extreme as on the shelf. Consistent with previous reports, we find the shelf sediments acted as intense fixed N recycling sites, whereas sediments within the core of the OMZ and deeper tended to behave as fixed N sinks.

2. Methods

2.1. Description of study area

The eastern tropical south Pacific is characterized by one of the most pronounced oxygen minimum zones (OMZ) in today's ocean. It is maintained by the combination of sluggish ocean circulation and enhanced microbial subsurface respiration due to high primary production and associated export of organic matter at the continental margin (e.g., Wyrtki, 1962; Brandt et al., 2015). At the Peruvian margin, elevated productivity is caused by coastal upwelling (Strub et al., 1998) sustained by alongshore equatorward trade winds and cyclonic wind-stress curl, both varying in strength seasonally. Highest productivity is observed between 5° and 15°S (Echevin et al., 2008). Nutrient–rich but oxygen poor Equatorial Subsurface Water (ESSW) is supplied to the upwelling region by the Peruvian-Chile Undercurrent (PCUC) flowing poleward along the upper continental slope and the shelf between 50 and 300m depth (Chaigneau et al., 2013). During its southward passage within the PCUC, the initially nitrate-rich ESSW becomes increasingly depleted in nitrogen, particularly

within the bottom boundary layer (Kalvelage et al., 2013; Thomsen et al., 2015). Below the PCUC, observations revealed the existence of a weak equatorward flow, the Chile-Peru Deep Coastal Current (CPDCC) (Chaigneau et al., 2013; Pietri et al., 2014) carrying cold and low-saline Antarctic Intermediate Water (AAIW) northward.

During the measurement program carried out on R/V Meteor cruise 92 from 6 January to 3 February 2013, moderate southeasterly winds prevailed along 12°S, typical for the austral summer season. Within about 55 km from the coast, ship-board measurements indicated average winds of 5 m s^{-1} with sustained periods of winds below 1 m s^{-1}. In the first two weeks of January 2013, elevated poleward alongshore velocities above 0.25 m s^{-1} were observed between 100 and 200 m depth associated with the PCUC, while the flow higher up on the shelf (<100m) was weak (Thomsen et al., 2015). Towards the end of January, the PCUC separated from the continental slope forming a subsurface anticyclonic eddy in February. The evolution of the flow and the associated cross-slope exchange of solutes due to the presence of the eddy are detailed in Thomsen et al. (2015).

During the observational period, water masses along the continental margin at the thermocline level and below were low-oxygen ESSW and AAIW. Their presence led to a rapid decrease of O_2-level with depth. Across the continental margin O_2 concentrations below the detection limit of the Winker titration (ca. 2 µM) were observed below ca. 30 to 50 m depth down to a water depth of ca. 500 m, at which point they gradually increased to about 50 µM at 1000 m (Figure 1).

The biogeochemistry of the sediments and water column of the Peruvian margin was investigated along a latitudinal depth transect at 12 °S from a water depth ranging from 74 m on the shelf to 989 m below the OMZ, equal to a horizontal distance of 80 km (Table 1, Fig. 1, Dale et al., 2015). Dissolved O_2 concentrations in the water column showed the presence of O_2-deficient water overlying the upper slope sediments, as described above.

Sediments on the upper continental slope and shelf off Peru between 11° and 15°S can be classified as fine grained, diatomaceous, organic carbon rich muds (> 5 wt %) (Suess et al., 1987). Sediment accumulation rates on the shallow shelf down to 100 m at 12°S are very high (0.45 cm yr^{-1}) decreasing to < 0.1 cm yr^{-1} below 200 m (Dale et al., 2015). Organic carbon is preferentially preserved in the OMZ with burial efficiencies exceeding 70 % (Dale et al., 2015). Sediments on the shelf and upper slope are covered with mats of the sulphide-oxidizing bacteria *Thioploca* and *Beggiatoa* (Levin et al., 2002; Mosch et al., 2012). Their biomass varies temporally depending on the redox potential of the overlying water column (Gutiérrez et al., 2008). At 12°S, mats completely covered the seafloor, with surface coverage decreasing down to 300 m (Dale et al., 2015). At the 409 m site, mats were absent and the surface 3 cm of sediments were instead characterized as foraminiferal ooze (Dale et al., 2015). Abundant nitrate-storing denitrifying foraminifera have been observed previously within the OMZ at 11°S and are suspected to play a major role in benthic N loss on the margin (Glock et al. 2013).

On the basis of bottom water O_2 distributions and sedimentary particulate organic carbon (POC) content, Dale et al. (2015) characterized the Peruvian margin at this latitude into 3 zones reflecting bottom water O_2 distributions and sedimentary POC content: (i) the shelf (< ca. 200 m, POC 5 to 10%, O_2 < detection limit (dl) at time of sampling) where non-steady state conditions are occasionally driven by periodic intrusion of oxygenated bottom waters (Levin et al., 2002; Gutiérrez et al., 2008), (ii) the core of the OMZ (ca. 200 to 500 m, POC 10 – 20%, O_2 < dl) where periodic intrusions of oxic bottom waters are less likely, and (iii) the deep stations below the OMZ (POC ≤ ca. 5% and O_2 > dl). We adopt the same notation in this work.

2.2. In situ flux benthic incubations to determine fluxes

Solute fluxes traversing the Peruvian OMZ at 12°S were determined using data measured in situ using two Biogeochemical Observatories BIGO I and BIGO II. These landers are described in detail by Pfannkuche & Linke (2003) and Sommer et al. (2009). Ten sampling sites were included in the programme (Fig. 1, Table 1). Sediments for geochemical analysis were sampled using a video-controlled multiple corer (MUC); these data are shown in Dale et al. (2015) and Dale et al. (2016).

Details of the lander operations at 12°S, as well as fluxes of dissolved inorganic carbon (DIC), are described by Dale et al. (2015). In brief, the BIGO observatories contained two circular flux chambers (internal diameter 28.8 cm, area 651.4 cm^2), herein referred to as chamber 1 (C1) and chamber 2 (C2). A TV–guided launching system allowed smooth emplacement of the observatories at selected sites on the sea floor. Four hours after the observatories were placed on the sea floor the chambers were slowly driven into the sediment (~ 30 cm h^{-1}). During this initial time period, the water inside the flux chamber was periodically replaced with ambient bottom water. After the chamber was fully driven into the sediment, the chamber water was again replaced with ambient bottom water to flush out solutes that might have been released from the sediment during chamber insertion. The water volume enclosed by the benthic chamber ranged from 7.8 to 16.3 L. To determine benthic fluxes, eight sequential water samples were removed periodically with glass syringes (volume of each syringe ~ 46 to 47 ml). The syringes were connected to the chamber using 1 m long Vygon tubes with a dead volume of 6.9 ml. Prior to deployment, these tubes were filled with distilled water and care was taken to avoid enclosure of air bubbles. An additional syringe water sampler (8 sequential samples) was used to monitor the ambient bottom water. The sampling ports for ambient bottom water were positioned about 30 – 40 cm above the sediment-water interface. For the measurement of the dinitrogen/argon ratio (N_2/Ar) water

samples were pumped in to 750 mm long glass tubes with an internal diameter of 4.6 mm (volume ~ 12.5 ml) using self-constructed underwater peristaltic pumps. Prior to deployment each glass tube was filled with distilled water, which was completely replaced by the sample without dilution. Four tubes were used to sample each chamber and the ambient bottom water.

The incubations were conducted for time periods of 28 h, defined by the time between the chamber was pushed into the sediment and the last syringe water sample was taken. Immediately after retrieval of the observatories, the water samples were transferred to the onboard cool room (8 °C) for further sample processing.

The O_2 concentration in each chamber and in the ambient bottom water was measured using optodes (Aanderaa Systems, Tengberg et al., 2006; Aanderaa Instruments, 2003). The precision of the sensors is better at lower concentrations (± 0.5 μM) than at higher concentrations of 300–500 μM (± 1 μM). The effect of salinity on the measured oxygen concentration was corrected internally by the optode using a salinity of 35. Pressure lowers the response of oxygen detection by about 4% per 100 bar pressure. As shown by Tengberg et al. (2006), this response is reversible and predictable. The effect of pressure on the oxygen concentration was compensated following the manufacturers recommendations (Aanderaa Instruments, 2003). For the calculation of the total oxygen uptake (TOU), the linear part of the O_2 time series after the start of the chamber incubation was used.

Geochemical fluxes were calculated from the linear increase or decrease of their concentrations with time. Negative fluxes denote uptake by the sediment whereas positive values indicate benthic release. The full set of data, including data points omitted from the flux calculations is shown in the Supplement.

2.3 Geochemical measurements

Measurements of NO_2^-, and NO_3^- in the water samples were performed on board using a QuAAtro autoanalyzer (Seal Analytical) with a detection limit of 30 and 5 nM, respectively, and a precision of 0.8 and 1.8 %. NH_4^+ and H_2S were measured on board using standard photometric techniques with a Hitachi U2800 photometer (Grasshoff et al., 1983). Sample aliquots were diluted with O_2–free artificial seawater prior to analysis where necessary. Detection limits for NH_4^+ and H_2S were 2 and 1 µM, respectively, with a precision of 5 and 3 µM.

Sedimentary N_2 release was measured by determining changes in the N_2/Ar ratio following the method of Kana et al. (1994). The N_2 release or uptake during the flux measurements was interpreted as representing the net N_2 production/consumption by denitrification, anammox and benthic N_2 fixation. Only natural N_2 fluxes were measured, that is, no ^{15}N labelled solutes were added to the chambers.

The water samples retrieved in the glass tubes by the observatories were connected the membrane inlet of the Quadrupol massspectrometer (GAM 200, IPI instruments, Bremen, Germany) without contamination by atmospheric nitrogen. Until and during the measurements, the glass tubes were kept in a cooling box under in situ temperature. The glass tubes were supported almost vertically and water samples were drawn into the membrane inlet using a peristaltic pump (Ismatec) at a constant flow rate of 1 to 2 ml min^{-1} for each series of measurements. Within the glass inlet, the water was sucked through a permeable silicone tube (length 40 mm, i. d.: 1.57 mm, Dow Corning Silastic tubing). The membrane inlet was kept in a Dewar vessel at in situ temperature, whose temperature was kept constant using a thermostat (Julabo F34).

Gas flow from the inlet to the mass spectrometer was supported with He supplied through a fused silica capillary (i.d. 100 µm). A cryo trap (ethanol at – 35° C) inline between the inlet

and the mass spectrometer was used to reduce water vapour. In order to control whether all ultrapure water inside the glass tubes was completely replaced with sample, the conductivity of the sample was measured inline using a micro flow cell (Amber Science Inc., Oregon, USA) and a conductivity meter (Model 3082, Amber Science, Oregon USA).

Concentrations of N_2 and Ar were obtained from ion currents at a mass to charge ratio 28 and 40. A Secondary Electron Multiplier was used as a detector. Instrument response time was less than 4 min. Calibration curves for the N_2 and Ar ion currents were constructed using air equilibrated filtered (0.2 µm) seawater, diluted seawater (50% and 75%) and distilled water. The dissolved N_2 and Ar concentrations of the saturated air equilibrated water standards were calculated using the solubility equations of Hamme and Emerson (2004). Before calculating the gas concentrations the ion currents were corrected for instrument drift. Calibrations were conducted before and after each measurement session.

2.4 Seafloor imaging

Sea floor imaging was conducted using a video camera attached to the MUC approximately 1 m above the seafloor. At each of the lander deployment sites at least one MUC cast was performed during which seafloor images were obtained.

3. Results

3.1. Seafloor imaging

Seafloor images confirmed that the sediments on the middle shelf and in the OMZ down to about 300 m hosted communities of mat-forming sulphur oxidizing bacteria visible to the naked eye (Fig. 2), *Thioploca* spp. and probably *Beggiatoa* spp. (Levin et al., 2002; Gutiérrez et al., 2008; Mosch et al., 2012). Video imaging of the seafloor during sediment sampling

using a TV-guided multiple corer (Dale et al., 2016) showed that mat coverage roughly decreased from 100 % at the shallowest station to around 40 % at 300 m where the bacteria formed patches of several decimetres in diameter. At 410 m water depth within the OMZ, no sulphur bacteria were visible on the sediment surface. Instead, exposed foraminiferal ooze was observed that contained high numbers of live nitrate-storing foraminifera (Dale et al., 2015; J. Cardich, unpub. data). Foraminiferal sands were also observed below the OMZ at 648 m. Attempts to sample the seafloor between these stations at 505 m were unsuccessful due to hard-ground. At the deepest sites >750 m, the sediment was bioturbated and colonized by epibenthic organisms.

3.2. DIN distributions

At the shallowest stations on the shelf (74 m and 101m water depth), NO_3^- and NO_2^- in the bottom water were close to depletion (Fig. 3). Bottom water NO_3^- steadily increased below 100 m to a maximum concentration of 45 µM at 760 m. Bottom water NO_2^- concentrations increased below 90 m and peaked at 10 µM at 190 m depth, before gradually decreasing towards near-detection limit at the lower edge of the OMZ at around 500 m. NH_4^+ concentrations were elevated in the water column on the shelf with highest concentrations of 2.1 µM. Below ca. 100 m, NH_4^+ concentrations were below detection limit. Bottom water H_2S concentrations determined from the lander sampling syringes were below detection limit at all stations (data not shown).

3.3. Benthic fluxes

All benthic concentration time series from which the fluxes were determined are shown in the Supplement. From the ten lander deployments along the 12°S transect, a maximum of 20

fluxes of each N species could be calculated from the concentration changes measured inside the benthic chamber (Table 2, Fig. 4). As expected from the very low or undetectable concentration of NO_3^- and NO_2^- in the bottom water at the shallowest station (74 m), benthic NO_3^- and NO_2^- fluxes were zero or non-determinable on the middle shelf. Sulphide was released from the sediment here with an average flux of 12.6 mmol m^{-2} d^{-1} (Table 2). At 101 m, NO_3^- was below detection limit in the chamber and no flux was measurable. No NO_2^- flux could be reliably determined either since NO_2^- was completely consumed inside the benthic chamber from 0.3 µM to zero after the second water sample was taken. Sulphide began to accumulate in the chamber as soon as NO_2^- disappeared, from which a potential flux of 4.3 to 5.3 mmol m^{-2} d^{-1} of H_2S was derived (Table 2). Similarly, despite moderate bottom water NO_3^- at 128 m, no flux could be determined due to rapid consumption inside the chamber. A very high NO_2^- uptake flux of -1.8 mmol m^{-2} d^{-1} was measurable due to high bottom water concentrations of 8 µM. Again, once NO_2^- had been completely consumed (after 20 h), H_2S accumulated with a potential flux of 4.2 mmol m^{-2} d^{-1}. This type of dynamic is shown more clearly in Fig. 10 in the companion paper (Dale et al., 2016) and the Supplement.

The highest NO_3^- flux of -3.3 mmol m^{-2} d^{-1} was calculated for the 142 m station on the outer shelf. Deeper within the OMZ, NO_3^- uptake remained elevated but decreased to < -1 mmol m^{-2} d^{-1} beyond the lower boundary of the OMZ. At the deepest station, NO_3^- was released in one chamber with a flux of 0.23 mmol m^{-2} d^{-1}. NO_2^- fluxes also tailed off strongly below the lower edge of the OMZ, and NO_2^- was released from the sediment at 0.08 mmol m^{-2} d^{-1} at the 409 m station with foraminiferal ooze. NO_2^- was below detection limit at the two deepest stations.

Benthic NH_4^+ release was exceptional on the shelf with fluxes up to 21.2 mmol m^{-2} d^{-1} at the shallowest station (Fig. 4b, Table 2). Fluxes decreased rapidly to ca. 6 mmol m^{-1} d^{-1} at 101 and 128 m. Weak or non-detectable NH_4^+ effluxes were determined from 307 m within the OMZ and down to the deeper sites.

N_2 release into the bottom water was very low on the shelf (<0.8 mmol N m^{-2} d^{-1}) down to 142 m. N_2 release correlated with the NO_3^- and NO_2^- fluxes and began to increase sharply at ca. 195 m. The highest N_2 release of 4.6 mmol N m^{-2} d^{-1} was determined for the core of the OMZ at 244 m water depth.

Dissolved oxygen was only detected at the two deepest stations below the OMZ where fluxes ranged from -0.5 to -1.6 mmol m^{-2} d^{-1} (Table 2).

4. Discussion

4.1. Benthic sulphide emissions

The DIN fluxes measured at 12°S were similar, or slightly higher, as those determined for 11°S in 2008 (RV Meteor cruise M77-1/2; Bohlen et al., 2011) (Table 2). A notable exception is the shelf. Maximum measured NH_4^+ fluxes at 12°S were five-fold higher than the reported flux of 3.7 mmol m^{-2} d^{-1} for 11°S (Bohlen et al., 2011). Moderate NO_3^- and NO_2^- fluxes of 1 to 3 mmol m^{-2} d^{-1} were also determined (Bohlen et al., 2011), whereas at 12 ^oS the fluxes were very low due to bottom waters depleted in NO_3^- and NO_2^-.

The environmental conditions encountered at 12°S were atypical for eastern boundary upwelling systems. To our knowledge, our in situ benthic flux measurements are the first under such extreme conditions on an open margin. The unusual geochemical features may have been driven by the near-stagnant circulation observed on the middle shelf. Moored current records from 80 m depth (not shown) indicated alongshore velocities of less than 0.04 m s^{-1} during the observational period. The lack of significant flow inhibits advection of nutrient-rich waters from the north into the region as well as isopycnal cross-shelf exchange processes.

The observations show that the sediments at the shallowest station on the shelf were releasing sulphide, possibly contributing to a sulphidic event in the water column analogous to the large event reported for the Peruvian OMZ shelf waters in January 2009 (Schunck et al., 2013). The event witnessed by these authors is the only one documented for this region, yet could re-occur if stagnation events in Peruvian OMZ become more frequent. Sulphidic conditions in surface sediments on the shelf appear to be common during the high-productivity season (Cardich et al., 2015). Clearly, the socio-economic impacts on local fishery and aquaculture industries would be devastating if benthic sulphide was released en masse. Our fluxes further show that the sediments have a high potential for sulphide release and begin to release sulphide as soon as NO_3^- and NO_2^- become depleted (c.f. Supplement and Fig. 10 in Dale et al., 2016). At the time of sampling, therefore, the sediments were still in a *Thioploca* state (sensu Gutiérrez et al., 2008), although the coupled benthic-pelagic system on the shelf was close to a tipping point between prevailing anoxic and euxinic conditions.

These dynamics were investigated in more detail by Dale et al. (2016) who combined porewater geochemistry with a non-steady state model to investigate how sediments with nitrate-storing bacterial communities respond to NO_3^- and NO_2^- depletion. The model predicted an almost immediate increase in sulphide fluxes when NO_3^- and NO_2^- become exhausted, as the benthic incubation data suggest. Their model showed that this was caused by a switch of organic matter mineralization at the sediment-water interface from denitrification to sulphate reduction. With limited availability of reactive iron to precipitate free sulphide (Noffke et al., 2012), the sulphide produced is rapidly lost to the water column. Observations and model results further demonstrated that the concentrations of nitrate stored with sulphur oxidizing bacteria decreased with a half life of days-weeks following bottom water stagnation (Dale et al., 2016). Therefore, despite almost complete coverage of the seafloor by sulphur oxidizing bacteria, the bacteria displayed a limited capacity to mitigate sulphide fluxes once NO_2^- and NO_3^- disappeared. It has also been shown previously that

prolonged starvation of electron acceptors and exposure to sulphide will decimate *Thioploca* communities and force the benthic system to a sulphidic state (Guitiérrez et al., 2008). More knowledge on the timing and controls of sulphide release from sediments is urgently required to be able to predict the benthic response to bottom water stagnation.

4.2. Excess benthic N flux on the shelf

The effect of depletion of bottom water NO_3^- and NO_2^- on the shelf at 12°S was quantified by calculating using a benthic N mass balance (ΣN, Fig. 5). This was determined by summing the average fluxes of N_2, NO_3^-, NO_2^-, NH_4^+ and NH_4^+ released during organic matter degradation ($NH_4^+{}_{amm}$) (Table 2, Fig. 5). The latter, shown in Fig. 4b, was derived from the rate of organic carbon degradation determined from the dissolved inorganic carbon efflux and measured C/N ratios of sedimentary organic, noting that carbonate dissolution makes a negligible contribution to DIC fluxes on the margin (Dale et al., 2015). Also considered is the production of fixed N due to N_2 fixation based on direct assays of nitrogenase activity by Gier et al. (2015) using the acetylene reduction technique and a conversion factor of 3 C_2H_4:1 N_2 (Capone et al., 2005; Orcutt et al., 2001). N_2 fixation rates were determined in samples retrieved by a multiple corer at six stations (70-1025 m) along the same depth transect and integrated over the upper 0-20 cm. We assume for now that N_2 is fixed as NH_4^+ (see below).

At steady-state, the sum of these fluxes should equal zero if burial of adsorbed NH_4^+ can be ignored. At the sites close to the lower boundary of the OMZ (409 m) and deeper, fluxes were approximately balanced to within ± 1 mmol m^{-2} d^{-1} (Fig. 5 red curve). However, the data show a very large N imbalance on the shelf, with an excess flux of 13 mmol m^{-2} d^{-1} at 74 m and 3 mmol m^{-2} d^{-1} at 101 m. The N balance was also variable on the outer shelf, with ΣN ranging from -2.8 to 2.5 mmol m^{-2} d^{-1}. For the main part, the shelf stations down to 200 m showed an excess of N leaving the sediment. Applying the same approach to DIN fluxes

measured at 11°S reveals a more balanced picture (Fig. 5, blue curve). This result should be treated cautiously since N_2 and $NH_4^+{}_{amm}$ fluxes at 11°S are modelled data, whereas the mass balance at 12°S is based on field observations only.

The strong N imbalance on the shelf at 12°S was due to an excess release of NH_4^+ above the fraction that can be supplied by ammonification. The most likely process that could drive this excess is DNRA by sulphur oxidizing bacteria (Guitiérrez et al., 2008; Bohlen et al., 2011; Mosch et al., 2012). N_2 fixation at 74 m (<0.5 mmol m^{-2} d^{-1}, Table 2) accounted for < 1 % of the NH_4^+ flux. Consequently, we estimate that DNRA at the shallowest station contributed up to 63 % (12.4 mmol m^{-2} d^{-1}) to the total NH_4^+ flux, with lower, yet still important, contributions at most of the other shelf stations (Fig. 4b). It should be noted that although N_2 fixation could account for an average of 17 % of the NH_4^+ flux at 142 m where ΣN showed a deficit, N_2 fixation is ten times too low to bring the N cycle back into balance.

At the shallowest stations where NO_3^- and NO_2^- were depleted, we propose that the imbalance in N fluxes was caused by filamentous sulphur bacteria relying on their internal NO_3^- and/or NO_2^- storage to maintain their activity levels during the period of bottom water stagnation. The internal NO_3^- reservoir is vast, with intracellular concentrations reaching 500 mM (e.g. McHatton et al., 1996). We determined porewater equivalent concentrations of 1 to 2 mM at the shelf stations at 12°S (Dale et al., 2016), demonstrating a decoupling of NO_3^-/NO_2^- uptake from the bottom water reservoirs. This strategy allows *Thioploca* and other nitrate-storing bacteria such as *Thiomargarita* spp. to survive in the absence of bottom water NO_3^- and NO_2^- (Otte et al., 1999; Schulz et al., 1999). The timing of internal NO_3^- consumption in relation to bottom water NO_3^- deficits has been addressed in the companion paper (Dale et al., 2016). At the deeper shelf stations, we speculate that the variability in ΣN could reflect a more general temporal decoupling of NO_3^- uptake and NH_4^+ due to natural fluctuations in bacterial biomass (Gutiérrez et al., 2008). Causes for this decoupling remain uncertain, but are most likely

related to the redox history of the bottom water as well as the rain rate of labile organic matter to the seafloor.

4.3. Excess benthic N flux in the OMZ

At the deep sediments within the OMZ down to ca. 400 m, ΣN again revealed an excess loss of N from the sediments of 2.5 to 4.1 mmol m^{-2} d^{-1} (Fig. 5). DNRA is of less importance here, in agreement with lower microbial mat coverage and low NH_4^+ fluxes. Although we cannot rule out temporal decoupling of NO_3^- uptake and NH_4^+ as described for the shelf, the flux data suggest that this imbalance rests with an excess flux of N_2 from the sediment because the uptake of oxidized N is insufficient to drive the high measured N_2 fluxes. A similar imbalance was observed in the anoxic Magdelena and Soledad basins on the Californian margin (Chong et al., 2012).

Measured abundances of nitrate-storing foraminifera (J. Cardich, unpub. data) along with the photographic evidence reveal a transition in the surface benthic microfauna community structure from bacterial mats at the shallow stations to foraminifera at the lower edge of the OMZ. There is accumulating evidence that benthic foraminifera are involved in dissimilatory pathways of the nitrogen cycle where NO_3^- is used as an electron acceptor during anaerobic respiration (Risgaard-Petersen et al., 2006; Pina-Ochoa et al., 2010). Similar to the sulphur bacteria, foraminifera can accumulate NO_3^- (Risgaard-Petersen et al., 2006; Pina-Ochoa et al., 2010). Due to their high population density in the Peruvian OMZ, it has been suggested that foraminifera play a key role in the sedimentary NO_3^- budget (Mallon et al., 2012). By combining abundances and species-specific denitrification rates available in the literature for the 11°S transect (RV Meteor cruise M77-1/2) it has been inferred that foraminifera are responsible for the total benthic NO_3^- loss at the shelf (80 m) and upper slope (250 m) (Glock et al., 2013). This has been confirmed at 12°S using the diagenetic model that accounts for

this N loss pathway (Dale et al., 2016). A very high foraminiferal contribution to total benthic denitrification of 60 % has also been observed in the Santa Barbara Basin (Bernhard et al., 2012). Low N_2 fluxes on the shelf (Fig. 4c) imply that these organisms were of minor importance for the benthic N turnover at the dense microbial mat sites, possibly due to the higher bacterial biomass outstripping the capacity of foraminifera to store and process nitrate.

We suggest that the excess N_2 fluxes in the OMZ are caused by a temporal decoupling of NO_3^- uptake and storage by denitrifying foraminifera, although we note that the contribution by nitrate-storing denitrifying bacteria is uncertain. At this stage, it cannot be substantiated whether this decoupling reflects the natural situation or an experiment artifact. However, because these sites are located deep within the OMZ and are subjected to less temporal variability in redox conditions than on the shelf, we suspect that the artificial depletion of NO_3^- in the chamber water during the incubation period could have led to enhanced N_2 fluxes. NO_3^- decreased from ca. 7 μM to undetectable levels inside the chamber at the 195 m site, and from ca. 20 μM to < 1 μM at the 244 m station (see Supplement). Such a rapid decrease in NO_3^- availability may have stressed the foraminiferal community, forcing them to more rapidly deplete their internal NO_3^- reservoir. A simple calculation shows that this hypothesis is consistent with the time-scale of the benthic lander deployment (28 h). Foraminifera abundance is highest in the surface centimetre (Cardich et al., 2012), such that the characteristic time for a molecule of N_2 to diffuse across the mean depth (0.5 cm) can be calculated from the equation $t = \pi L^2/4D$, where L is mean diffusive path length and D is the in situ diffusion coefficient of N_2 corrected for tortuosity. For D = 300 cm^2 yr^{-1} (Boudreau, 1997), $t = \pi \cdot 0.5^2/4 \cdot 300$ = ~6 hours. A sudden increase in denitrification by foraminifera would, therefore, be detectable in the N_2 concentrations determined in water samples withdrawn from the chamber for gas analysis every 6 hours. These artefacts could be avoided in future by maintaining NO_3^- concentrations inside the chambers at ambient bottom water levels.

5. Conclusions

In contrast to the common perception that continental margin sediments in general represent major sinks for fixed nitrogen, Peruvian shelf and upper slope sediments are strong source of reduced fixed N via the activity of sulphur oxidizing bacteria performing DNRA. Although a few previous studies have highlighted the significance of DNRA, this process is generally neglected in regional N budgets and biogeochemical models. Yet, DNRA could have important feedbacks on productivity and the N balance of oxygen deficient regions depending on whether the benthic NH_4^+ reaches the euphotic zone to stimulate primary productivity or whether it is oxidized anaerobically in the water column.

Temporal variability in the bottom water redox-conditions due to varying strength and direction of water circulation on the upper slope has been shown to lead to strong imbalances in the benthic N turnover. During periods of bottom water NO_3^- and NO_2^- depletion, storage of electron acceptors within sulphur bacteria and foraminifera becomes an important source of oxidative power for sustaining the respiratory activity of these organisms, resulting in a temporal decoupling between NO_3^- uptake from the bottom water and benthic fluxes of NH_4^+ and N_2. These periods, which are only just beginning to be understood from a benthic perspective, can be expected to strongly affect benthic-pelagic nutrient inventories on regional scales.

Acknowledgements

We are grateful for the support of the officers and crew of RV 'Meteor' during cruise M92. Many thanks are due to A. Petersen, M. Türk and S. Cherednichenko for their assistance in deploying the landers. We thank B. Domeyer, S. Kriwanek, A. Bleyer, R. Suhrberg, S. Trinkler and V. Thoenissen for biogeochemical analyses on board and in the home laboratory. We highly appreciate the constructive comments of two anonymous reviewers, which helped to improve this manuscript. This work is a contribution of the Sonderforschungsbereich 754 "Climate – Biogeochemistry Interactions in the Tropical Ocean" (www.sfb754.de) which is supported by the Deutsche Forschungsgemeinschaft.

References

Aanderaa Instruments AS (2003). TD 218 Operating manual oxygen optode 3830 and 3930.

Berelson, W. M., D. E. Hammond, and K. S. Johnson, K. S. (1987), Benthic Fluxes And The Cycling Of Biogenic Silica And Carbon In 2 Southern–California Borderland Basins, *Geochim. Cosmochim. Acta, 51(6),* 1345–1363.

Bernhard, J. M., Casciotti, K. L., McIlvin, M. R., Beaudoin, D. J., Visscher, P. T., Edgcomb, V. P. (2012) Potential importance of physiologically diverse benthic foraminifera in sedimentary nitrate storage and respiration, J. Geophys. Res., 117, G03002, doi:10.1029/2012JG001949, 2012a.

Bohlen, L., Dale, A.W., Sommer, S., Mosch, T., Hensen, C., Noffke, A., Scholz, F., Wallmann, K. (2011) Benthic nitrogen cycling traversing the Peruvian oxygen minimum zone. Geochim Cosmochim Acta, 75, 6094-6111. doi:10.1016/j.gca.2011.08.010

Boudreau, B. P. (1996) A method-of-lines code for carbon and nutrient diagenesis in aquatic sediments, *Comput. Geosci*., 22(5), 479–496.

Brandt, P., H. W. Bange, D. Banyte, M. Dengler, S.-H. Didwischus, T. Fischer, R. J. Greatbatch, J. Hahn, T. Kanzow, J. Karstensen, A. Koertzinger, G. Krahmann, S. Schmidtko, L. Stramma, T. Tanhua, and M. Visbeck (2015), On the role of circulation and mixing in the ventilation of oxygen minimum zones with a focus on the Eastern Tropical North Atlantic, *Biogeosciences*, 12 (2), 489-512, doi:10.5194/bg-12-489-2015.

Brüchert, V., Jørgensen, B.B., Neumann, K., Riechmann, D., Schlösser, M., Schulz, H.N. (2003). Regulation of bacterial sulfate reduction and hydrogen sulfide fluxes in the central Namibian coastal upwelling zone. *Geochim Cosmochim Acta* 67: 4505–4518.

Capone, D. G. (1993). Determination of nitrogenase activity in aquatic samples using the acetylene reduction procedure. In P. F. Kemp, B. F. Sherr, E. B. Sherr, & J. J. Coles (Eds.), *Handbook of methods in aquatic microbial ecology* (pp. 621–631). Boca Raton: CRC Press LLC.

Capone, D. G., Burns, J. a., Montoya, J. P., Subramaniam, A., Mahaffey, C., Gunderson, T., Carpenter, E. J. (2005). Nitrogen fixation by *Trichodesmium* spp.: An important source of new nitrogen to the tropical and subtropical North Atlantic Ocean. *Glob. Biogeochem. Cy.*, *19*, 1–17.

Cardich, J., Morales, M., Quipúzcoa, L., Sifeddine, A., Gutiérrez, D. (2012) Benthic foraminiferal communities and microhabitat selection on the continental shelf off central Peru. In: Altenbach, A.V., Bernhard, J.M., Seckbach, J. (eds) Anoxia: Evidence for eukaryote survival and paleontological strategies, Vol 21. Springer Science+Business Media, 323-340.

Cardich, J., Gutiérrez, D., Romero, D., Pérez, A., Quipúzcoa, L., Morales, M., Marquina, R., Yupanqui, W., Solís, J., Carhuapoma, W., Sifeddine, A. (2015) Calcareous benthic foraminifera associated to geochemical conditions in the upper central Peruvian margin: control by pore water redox and sedimentary organic matter. *Mar. Ecol. Prog. Ser.*, 535, 63-87, doi: 10.3354/meps11409

Chaigneau, A., Dominguez, N., Eldin, G., Vasquez, L., Flores, R., Grados, C. and Echevin, V.: Near-coastal circulation in the Northern Humboldt Current System from shipboard ADCP data, *J. Geophys. Res-Oceans*, 118, 5251-5266, doi: 10.1002/jgrc.20328, 2013.

Dale, A. W., S. Sommer, L. Bohlen, T. Treude, V. J. Bertics, H. W. Bange, O. Pfannkuche, T. Schorp, M. Mattsdotter, and K. Wallmann (2011) Rates and regulation of nitrogen cycling in seasonally hypoxic sediments during winter (Boknis Eck, SW Baltic Sea): sensitivity to environmental parameters. *Estuar. Coast. Shelf Sci.*, 95, 14-28, doi: 10.1016/j.ecss.2011.05.016.

Dale, A. W., Sommer, S., Lomnitz, U., Montes, I., Treude, T., Liebetrau, V., Gier, J. , Hensen, C., Dengler, M., Stolpovsky, K., Bryant, L. D., & Wallmann, K. (2015) Organic carbon production, mineralisation and preservation on the Peruvian margin. *Biogeosciences* 12, 1537-1559.

Dale, A. W., S. Sommer, Lomnitz, U., Bourbonnais, A., and K. Wallmann (2016) Biological nitrate transport in sediments on the Peruvian margin mitigates benthic sulfide emissions and drives pelagic N loss during stagnation events. *Deep Sea Res.*, in press.

Devol, A. H. (2015) Denitrification, anammox, and N_2 production in marine sediments. *Annual Review of Marine Science* 7, 403-423.

Devol, A. H., and J. P. Christensen (1993), Benthic Fluxes And Nitrogen Cycling In Sediments Of The Continental–Margin Of The Eastern North Pacific, *J. Mar. Res., 51(2)*, 345–372, doi:10.1357/0022240933223765.

Echevin, V., Aumont, A., Ledesma, J. and Flores, G.: The seasonal cycle of surface chlorophyll in the Peruvian upwelling system: A modelling study, *Prog. Oceanogr*, 79, 167-176, doi: 10.1016/j.pocean.2008.10.026, 2008.

Ferdelman T.G., Lee, C., Pantoja, S., Herder, J., Bebout, B.M., Fossing, H. (1997) Sulfate reduction and methanogenesis in a Thioploca-dominated sediment off the coast of Chile. Geochim. Cosmochim. Acta, 61, 3065-3079.

Fossing, H., V. A. Gallardo, B. B. Jørgensen, M. Hüttel, L. P. Nielsen, H. Schulz, D. E. Canfield, S. Forster, R. N. Glud, J. K. Gundersen, J. Küver, N. B. Ramsing, A. Teske, B. Thamdrup, and O. Ollua (1995), Concentration and transport of nitrate by the mat–forming sulphur bacterium Thioploca, *Nature, 374*, 713–715, doi:10.1038/374713a0.

Gallardo, V. A. (1977), Large benthic microbial communities in sulphide biota under Peru–Chile Subsurface Countercurrent, *Nature, 268*, 331–332, doi:10.1038/268331a0.

Gallardo, V. A., E. Klingelhoeffer, W. Arntz, and M. Graco (1998), First report of the bacterium Thioploca in the Benguela ecosystem off Namibia, *J. Mar. Biol. Assoc. UK, 78(3),* 1007–1010, doi: 10.1017/S0025315400044945.

Gier, J., Sommer, S., Löscher, C.R., Dale, A.W., Schmitz-Streit, R.A., Treude, T. (2015) Nitrogen fixation in sediments along a depth transect through the Peruvian oxygen minimum zone. *Biogeosciences Discussions*, to appear online shortly.

Glock, N., Schönfeld, J., Eisenhauer, A., Hensen, C., Mallon, J., Sommer,S. (2013) The role of benthic foraminifera in the benthic nitrogen cycle of the Peruvian oxygen minimum zone. Biogeosciences, 10, 4767-4783, doi:10.5194/bg-10-4767-2013.

Grasshoff, K., M. Ehrhardt, and K. Kremmling (1983), *Methods of Seawater Analysis*, Verlag Chemie GmbH, Weinheim, Germany.

Gruber N. (2004) The dynamics of the marine nitrogen cycle and its influence on atmospheric CO_2 variations. In "Carbon-Climate Interactions", T. Oguz and M. Follows, editors, NATO ASI series.

Gutiérrez, D., E. Enriquez, S.Purca, L. Quipuzcoa, R. Marquina, G. Flores, and M. Graco (2008), Oxygenation episodes on the continental shelf of central Peru: Remote forcing and benthic ecosystem response, *Progr. Oceanogr., 79(2–4),* 177–189, doi:10.1016/j.pocean.2008.10.025.

Hamme, R.C., Emerson S.R. (2004) The solubility of neon, nitrogen and argon in distilled water and seawater. Deep-Sea Res I, 51, 1517-1528.

Hartnett, H. E., and A. H. Devol (2003), Role of a strong oxygen–deficient zone in the preservation and degradation of organic matter: A carbon budget for the continental margins of northwest Mexico and Washington State, *Geochim. Cosmochim. Acta, 67(2),* 247–264, doi:10.1016/S0016–7037(02)01076–1.

Jørgensen, B. B., and V. A. Gallardo (1999), Thioploca spp.: filamentous sulfur bacteria with nitrate vacuoles, *FEMS Microbiology Ecology, 28(4),* 301–313, doi: 10.1111/j.1574–6941.1999.tb00585.x.

Jørgensen, B. B., and D. C. Nelson (2004), Sulfide oxidation in marine sediments: Geochemistry meets microbiology, in *Sulfur Biogeochemistry – Past and present*, edited by J. P. Amend, K. J. Edwards, and T. W. Lyons, pp. 63–81, Geological Society of America Special Paper, 379.

Kalvelage, T., Lavik, G., Lam, P., Contreras, S., Arteaga, L., Loescher, C. R., Oschlies, A., Paulmier, A., Stramma, L., & Kuypers, M. M. M., 2013, Nitrogen cycling driven by organic matter export in the South Pacific oxygen minimum zone, Nature Geoscience, v. 6, no. 3, p. 228-234.

Kana, T.M., Darkangelo, C., Hunt M.D., Oldham, J.B., Bennett, G.E., Cornwell, J.C. (2012) Membrane inlet mass spectrometer for rapid high-precission determination of N_2, O_2, and Ar in environmental water samples. Anal. Chem., 66, 4166-4170.

Lam, P., G. Lavik, M. M. Jensen, J. van de Vossenberg, M. Schmid, D. Woebken, D. Gutiérrez, R. Amann, M. S. M. Jetten, M. M. M. Kuypers (2009), Revising the nitrogen cycle in the Peruvian oxygen minimum zone. *PNAS*, 106, 4752–4757.

Levin L. A., D. Gutiérrez, A. Rathburn, C. Neira, J. Sellanes, P. Muñoz, V. Gallardo, and M. Salamanca (2002), Benthic processes on the Peru margin: a transect across the oxygen minimum zone during the 1997–98 El Niño, *Progr. Oceanogr., 53(1),* 1–27, doi:10.1016/S0079–6611(02)00022–8.

Mallon, J., Glock, N., Scho□nfeld, J. (2012) The response of benthic foraminifera to low-oxygen conditions of the Peruvian oxygen minimum zone. Anoxia, 305–321.

McHatton, S., Barry, J.P., Jannasch, H.W., Nelson, D.C. (1996). High nitrate concentrations in vacuolate autotrophic marine Beggiatoa spp. Appl. Environ. Microbiol.,62, 954–958.

Middelburg, J. J., K. Soetaert, P. M. J. Herman, and C. H. R. Heip (1996), Denitrification in marine sediments: A model study, *Global Biogeochem. Cycles*, *10*, 661–673.

Mosch, T., Sommer, S., Dengler, M., Noffke, A., Bohlen, L., Pfannkuche, O., Liebetrau, V., Wallmann, K. (2012) Factors influencing the distribution of epibenthic megafauna across the Peruvian oxygen minimum zone. Deep-Sea Res. I, 68, 123-135. doi.org/10.1016/j.dsr.2012.04.014

Noffke, A., Hensen, C., Sommer, S., Scholz, F., Bohlen, L., Mosch, T., Graco, M., & Wallmann, K. (2012) Benthic iron and phosphorus fluxes across the Peruvian oxygen minimum zone. *Limnology and Oceanography* 57, 851-867.

Noffke, A., Sommer, S., Dale, A. W., Hall, P. O. J., & Pfannkuche, O. Benthic nutrient fluxes in the Eastern Gotland Basin (Baltic Sea) with particular focus on microbial mat ecosystems. Journal of Marine Systems 158, 1-12. 2016.

Orcutt, K. M., Lipschultz, F., Gundersen, K., Arimoto, R., Michaels, A. F., Knap, A. H., Gallon, J. R. (2001). A seasonal study of the significance of N_2 fixation by Trichodesmium spp. at the Bermuda Atlantic Time-series Study (BATS) site. *Deep Sea Research Part II: Topical Studies in Oceanography*, *48*(8-9), 1583–1608.

Otte, S., J. G. Kuenen, L. P. Nielsen, H. W. Paerl, J. Zopfi, H. N. Schulz, A. Teske, B. Strotmann, V.A. Gallardo, B. B. Jørgensen (1999), Nitrogen, carbon, and sulfur metabolism in natural Thioploca samples, *Appl. Environmental. Microb.*, *65(7)*, 3148–3157.

Pfannkuche O, Linke P (2003) GEOMAR landers as long-term deep-sea observatories. *Sea Technology*, 44, 50-55.

Pietri, A., V. Echevin, P. Testor, A. Chaigneau, L. Mortier, C. Grados, and A. Albert (2014), Impact of a coastal trapped wave on the near-coastal circulation of the Peru upwelling system from glider data, *J. Geophys. Res. Oceans*, 119, 2109–2120, doi:10.1002/2013JC009270.

Pinã-Ochoa, E., Høgslund, S., Geslin, E., Cedhagen, T., Revsbech, N. P., Nielsen, L. P., Schweizer, M., Jorissen, F., Rysgaard, S., and Risgaard-Petersen, N. (2010) Widespread occurence of nitrate storage and denitrification among Foraminifera and *Gromiida*. P.Natl. Acad. Sci. USA, 107, 1148–1153, 2010.

Prokopenko, M. G., Hirst, M. B., De Brabandere, L., Lawrence, D. J. P., Berelson, W. M., Granger, J., Chang, B. X., Dawson, S., Crane III, E. J., Chong, L., Thamdrup, B., Townsend-Small, A., & Sigman, D. M. Nitrogen losses in anoxic marine sediments driven by Thioploca–anammox bacterial consortia. Nature, 500, 194-198. 2013.

Risgaard-Petersen, N., Langezaal, A. M., Ingvardsen, S., Schmid, M. C., Jetten, M. S., Op den Camp, H. J. M., Derksen, J. W. M., Pinã-Ochoa, E., Eriksson, S. P., Nielsen, L. P., Revsbech, N. P., Cedhagen, T., and van der Zwaan, G. J.: Evidence for com- plete denitrification in a benthic foraminifer, Nature, 443, 93–96, 2006.

Schmaljohann, R., M. Drews, S. Walter, P. Linke, U. von Rad, and J. F. Imhoff (2001), Oxygen–minimum zone sediments in the northeastern Arabian Sea off Pakistan: a habitat for the bacterium Thioploca, *Mar. Ecol. Prog. Ser, 211*, 27–42.

Schulz, H.N., Brinkhoff, T., Ferdelman, T.G., Hernánndez Mariné, M., Teske, A., Jørgensen, B.B. (1999) Dense populations of a giant sulphur bacterium in Namibian Shelf sediments. Science, 284, 493-495.

Schunck,H., and 15 others (2013) Giant Hydrogen Sulfide Plume in the Oxygen Minimum Zone off Peru Supports Chemolithoautotrophy. PLoS ONE 8(8): e68661. doi:10.1371/journal.pone.0068661

Sommer, S., P. Linke, O. Pfannkuche, T. Schleicher, J. Schneider v. Deimling, A. Reitz, M. Haeckel, S. Flögel, and C. Hensen (2009), Seabed methane emissions and the habitat of frenulate tubeworms on the Captain Arutyunov mud volcano (Gulf of Cadiz), *Mar. Ecol. Prog. Ser., 382*, 69–86, doi: 10.3354/meps07956.

Stramma, L., Johnson, G. C., Sprintall, J., & Mohrholz, V. (2008) Expanding oxygen-minimum zones in the tropical oceans. *Science* 320, 655-658.

Strub, P.T., Mesias, J.M., Montecino, V., Rutlant, J. and Salinas, S. (1998) Coastal ocean circulation off Western South America, in: *The Global Coastal Ocean*, edited by: Robinson, A.R., Brink, K.H., 273–314.

Suess, E., L. D. Kulm, and J. S. Killingley (1987), Coastal upwelling and a history of organic–rich mudstone deposition off Peru, in *Marine Petroleum Source Rocks*, edited by J. Brooks, and A. J. Fleet, pp. 181–197, Geological Society Special Publication No. 22.

Tengberg, A., J. Hovdenes, H. J. Andersson, O. Brocandel, R. Diaz, D. Hebert, T. Arnerich, C. Huber, A. Körtzinger, A. Khripounoff, F. Rey, C. Rönning, J. Schimanski, S. Sommer, and A. Stangelmayer (2006), Evaluation of a lifetime-based optode to measure oxygen in aquatic systems, *Limnol. Oceanogr: Methods*, 4, 7-17.

Teske, A. & Nelson, D.C. (2006) The genera Beggiatoa and Thioploca. Prokaryotes. 6, 784-810.

Teske A (2010) Cryptic links in the ocean. Science, 330, 1326-1327.

Thamdrup, B., Canfield, D.E. (1996) Pathways of carbon oxidation in continental margin sediments off central Chile. Limnol. Oceanogr., 41, 1629-1650.

Thomsen, S., T. Kanzow, G. Krahmann, R. J. Greatbatch, M. Dengler and G. Lavik (2016) The formation of a subsurface anticyclonic eddy in the Peru-Chile Undercurrent and its impact on the near-coastal distribution of salinity and oxygen, *J. Geophys. Res. Oceans*, 121, 476–501.

Woulds, C., M. C. Schwartz, T. Brand, G. Cowie, G. Law, and S. Mowbray (2009) Porewater nutrient concentrations and benthic nutrient fluxes across the Pakistan margin OMZ, *Deep–Sea Research II*, 56(6–7), 333–346, doi:10.1016/j.dsr2.2008.05.034.

Wyrtki, K. (1962) The oxygen minima in relation to ocean circulation, *Deep-Sea Res.*, 9, 11-23, doi:10.1016/0011-7471(62)90243-7.

Zopfi, J., T. Kjær, L. P. Nielsen, and B. B. Jørgensen (2001), Ecology of Thioploca spp.: Nitrate and sulfur storage in relation to chemical microgradients and influence of Thioploca spp. on the sedimentary nitrogen cycle, *Appl. Environ. Microbiol., 67(12)*, 5530–5537, doi: 10.1128/AEM.67.12.5530–5537.2001.

Figure captions

Fig. 1: (a) Bathymetry and benthic sampling locations (triangles) on the Peruvian margin at 12°S during January 2013. (b) Cross-section of dissolved oxygen concentrations (μM) measured using the CTD sensor calibrated against Winkler titrations (detection limit 5 μM). The positions of the CTD casts are indicated by vertical lines diamonds. Deployment sites of the benthic landers (BIGO) are shown as red triangles.

Fig. 2: Photographic images of sulfide-oxidizing microbial mats covering surface sediments at 103, 145 and 305 m water depth, taken using a camera installed on the multiple-corer. The white bars denote a distance of ca. 50 cm. A weight hanging ca. 1.5 m from the bottom of the multiple-corer can be seen in the images.

Fig. 3: Distributions of (a) nitrate, (b) nitrite, and (c) ammonium across the margin at 12°S, reconstructed from CTD casts taken during January 2013. The white contours show the potential density (kg m^{-3}). The positions of the CTD casts are indicated by vertical lines diamonds. Deployment sites of the benthic landers are shown as black triangles.

Fig. 4: Benthic fluxes (mmol m^{-2} d^{-1} of N) of (a) nitrate (black) and nitrite (red), (b) ammonium (black), and (c) dinitrogen across the margin at 12°S. Negative fluxes denote uptake by the sediments. Red, blue and green curves in (b) correspond to calculated fluxes due to ammonification, N_2 fixation and DNRA, respectively (see Discussion). Error bars correspond to minimum and maximum values and symbols are the mean values (n=2). Note that water depth increases from left to right.

Fig. 5: Benthic N mass balance (ΣN) for 12°S (red) and 11°S (blue). Positive values indicate a loss from the sediments and excess N flux to the water column, and negative values indicate excess N uptake by the sediments (units mmol m^{-2} d^{-1} of N). The N fluxes for the mass balance at 11°S are provided in Table 1. Note that water depth increases from left to right.

Supplemental Fig. S1a,b

S1a,b: Time-series concentrations of different chemical species measured during chamber flux measurements with BIGO I and BIGO II during the R/V Meteor cruise M92 along a depth transect at 12°S off Peru. Measurements in Chamber 1, Chamber 2 and the bottom water are represented by black circles, white circles and crosses respectively. For the oxygen plots continuous measurements in Chamber 1, Chamber 2 and the bottom water are represented by thick black, grey and thin black lines respectively. The abbreviation bdl indicates below detection limit.

Fig. 1

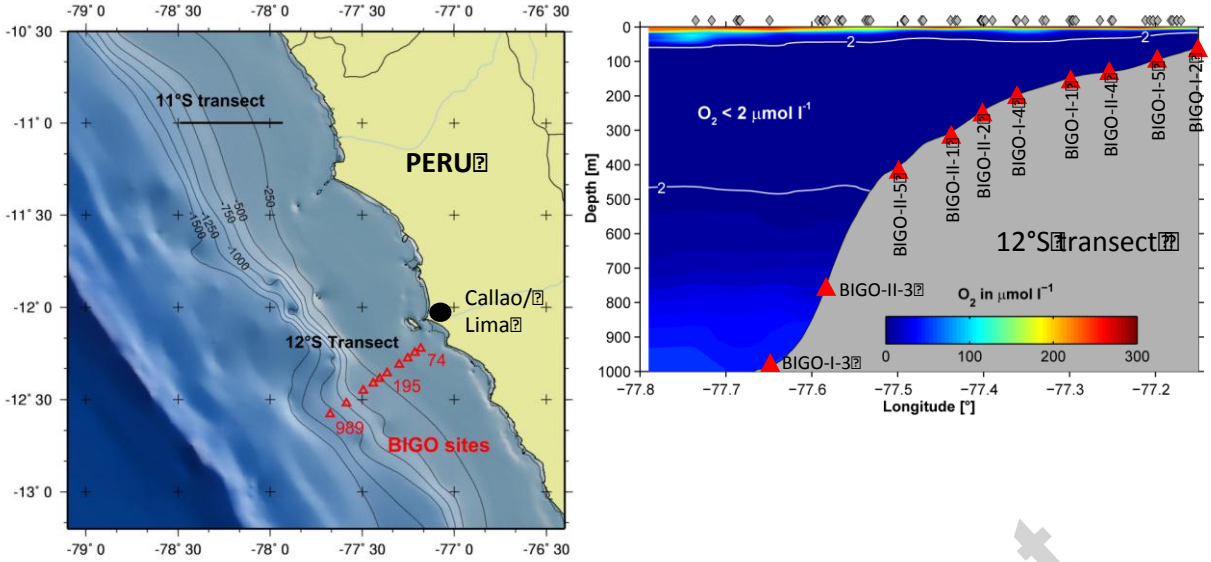

Fig. 2

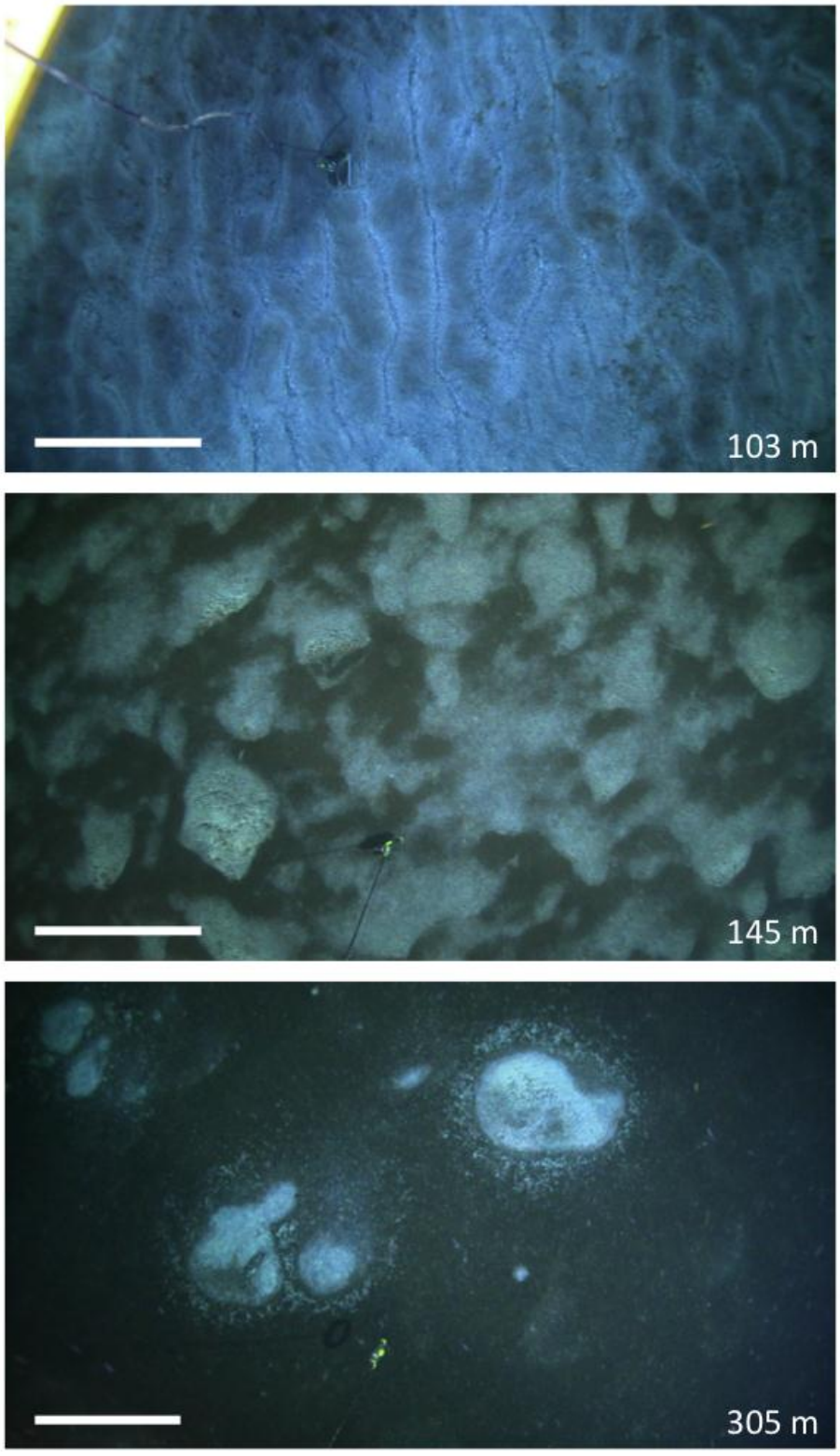

Fig. 3

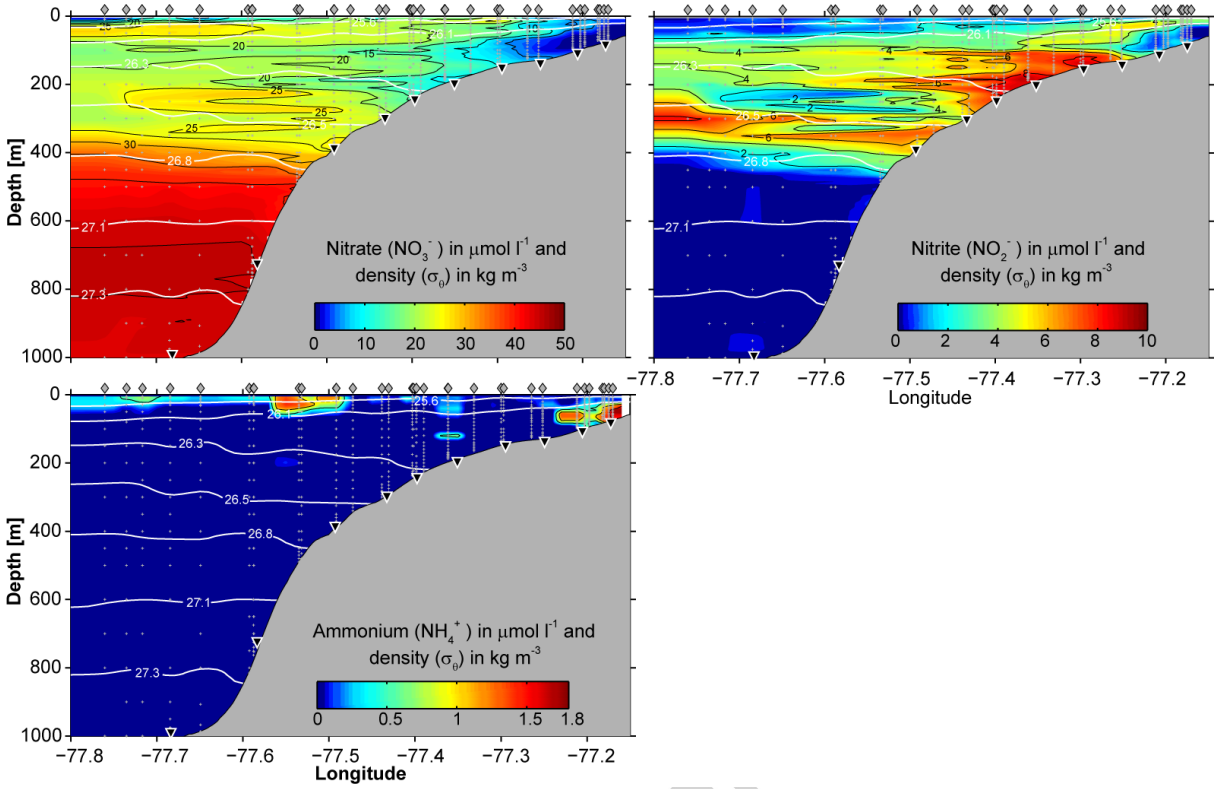

Fig. 4

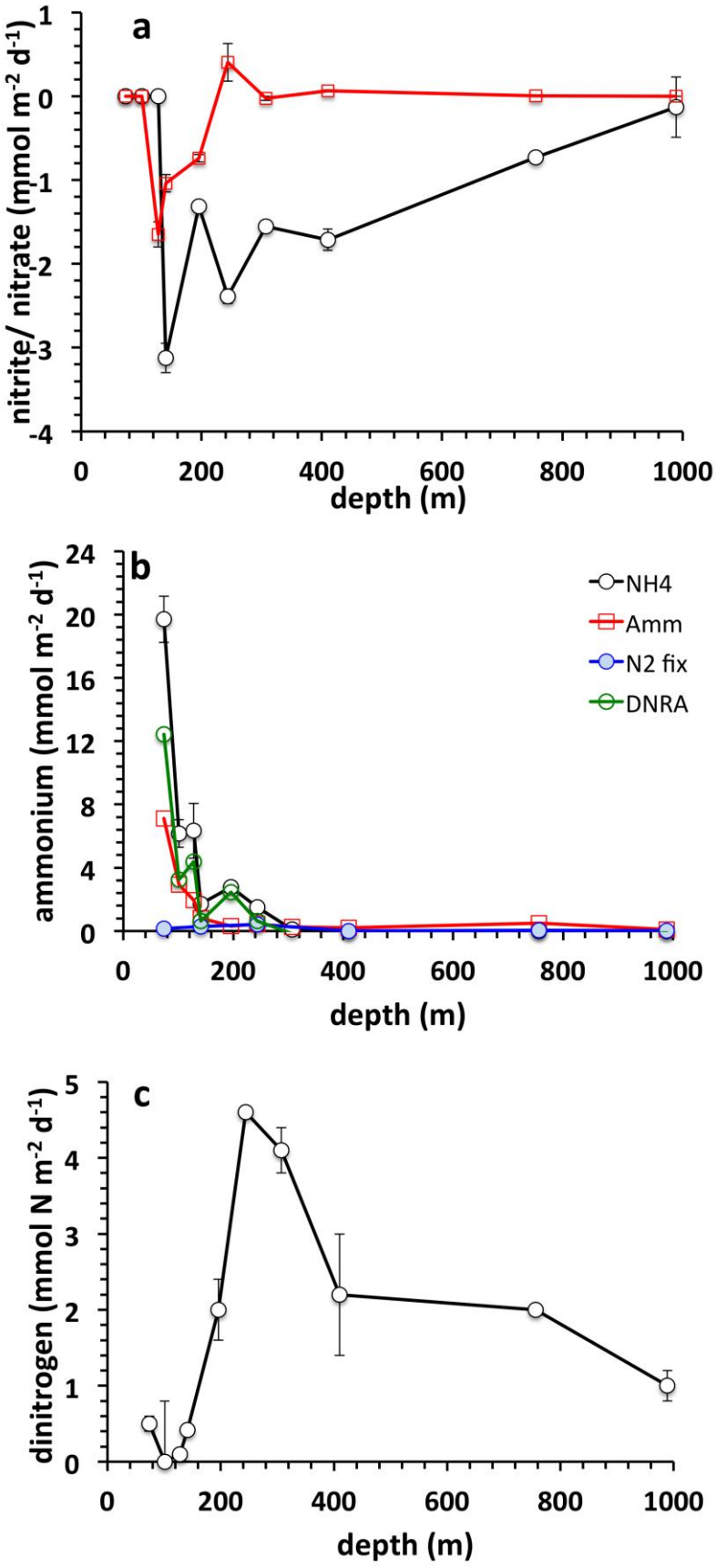
a
nitrite/ nitrate (mmol m-2 d-1)
1
0
-1
-2
-3
-4
0
200
400
600
800
1000
depth (m)
b
ammonium (mmol m-2 d-1)
24
20
16
12
8
4
0
NH4
Amm
N2 fix
DNRA
0
200
400
600
800
1000
depth (m)
c
dinitrogen (mmol N m-2 d-1)
5
4
3
2
1
0
0
200
400
600
800
1000
depth (m)

Fig.5

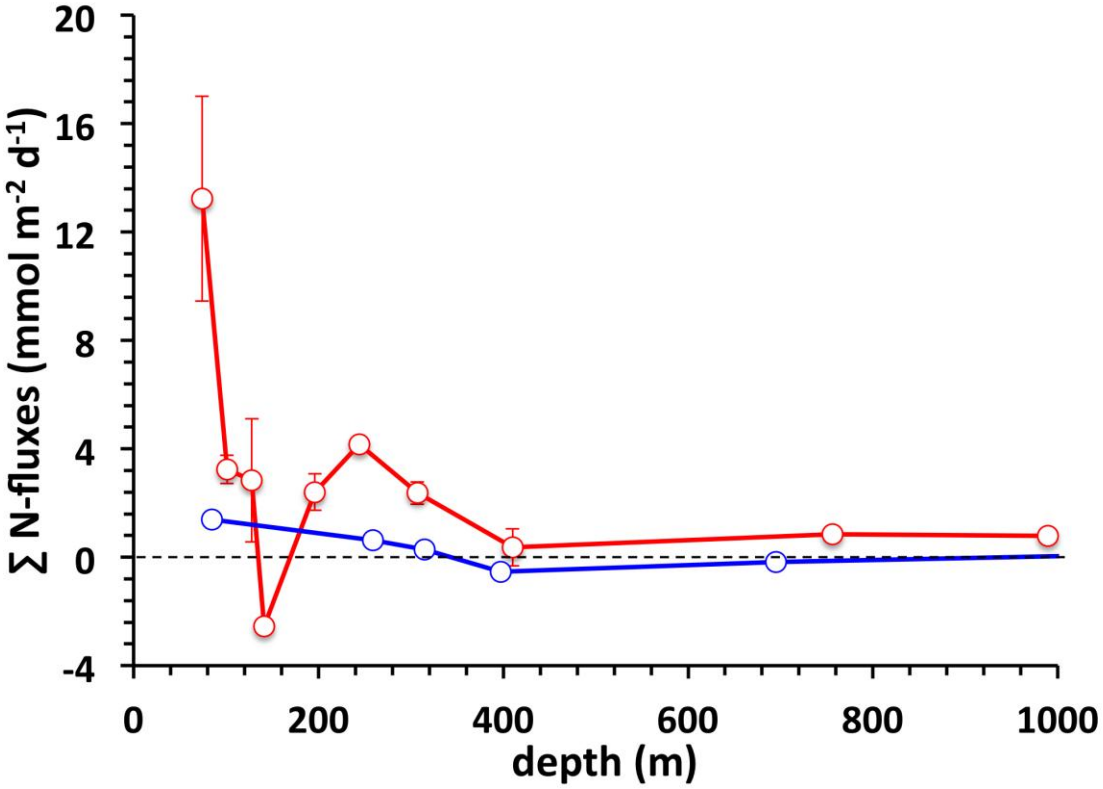

Tables

Table 1: Station and deployment data of the Biogeochemical Observatories I and II (BIGO) along a depth transect at 12°S off Peru

Instrument [a]	Date	Latitude (S)	Longitude (W)	Depth (m)	Habitat [b]
BIGO-I-2	15.01.2013	12°13.506’	77°10.793’	74	mats
BIGO-I-5	27.01.2013	12°14.898’	77°12.705’	101	mats
BIGO-II-4	20.01.2013	12°16.686’	77°14.995’	128	mats
BIGO-I-1	11.01.2013	12°18.711’	77°17.803’	142	mats
BIGO-I-4	23.01.2013	12°21.502’	77°21.712’	195	mats
BIGO-II-2	12.01.2013	12°23.301’	77°24.284’	244	mats
BIGO-II-1	08.01.2013	12°24.905’	77°26.295’	306	-
BIGO-II-5	24.01.2013	12°27.207’	77°29.517’	409	foraminifera
BIGO-II-3	16.01.2013	12°31.366’	77°34.997’	756	-
BIGO-I-3	19.01.2013	12°34.911’	77°40.365’	989	-

[a] The Roman numeral of the BIGO code denotes the lander used and the Arabic numeral is the deployment number of that lander.
[b] Predominant biota on the sediment surface visible to the naked eye. Mats denotes the presence of sulphide oxidizing microbial mats inside the flux chamber, foraminifera denotes the presence of foraminiferal sands on the sediment surface, and ‘-‘ indicates plain sediment surface without conspicuous mats or foraminiferal communities.

Table 2: In situ benthic fluxes, derived fluxes of DIC and rates of ammonification ($NH_4^+{}_{amm}$), DNRA and measured depth-integrated N_2 fixation rates (N_{2fix}) for chamber 1 (C1) and chamber 2 (C2) of each lander. All N-based data are in units of mmol N m^{-2} d^{-1}, TOU is in mmol O_2 m^{-2} d^{-1} and H_2S is in mmol H_2S m^{-2} d^{-1}. Flux uncertainty at 12°S is given as the standard error determined from the error in the slope of the concentration time series. Negative and positive fluxes indicate uptake and release from the seabed, respectively. bdl = below detection limit and empty cells indicate that no measurements were made. Fluxes are not determinable (nd) if the standard error is larger than the flux due to very low fluxes or data scatter.

Lander		Depth (m)	NO_3^-	NO_2^-	NH_4^+	N_2	H_2S [a]	TOU	DIC [b]	$NH_4^+{}_{amm}$ [c]	DNRA [d]	N_{2fix} [e]
Meteor cruise M92, 12°S, Jan/Feb 2013												
BIGO-I-2	C1	74	bdl	bdl	18.2±1.5	0.4	13.7±2.0	bdl	86.4±0.7	9.33	8.8	0.15
	C2		bdl	bdl	21.2±1.5	0.6	11.3±1.1	bdl	45.3±0.5	4.89	16.1	
BIGO-I-5	C1	101	bdl	nd [f]	7.1±0.7	-0.8	5.3±0.3*	bdl	23.4±0.5	2.48	4.6	
	C2		bdl	nd [f]	5.3±0.9	0.8	4.3±0.4*	bdl	31.8±0.5	3.37	1.9	
BIGO-II-4	C1	128	nd [g]	-1.80±0.2	8.1±1.2	0.2	4.2±1.6*	bdl	13.9±0.4	1.33	6.7	
	C2		nd [g]	-1.50±0.1	4.6±0.4	0.0	nd	bdl	26.9±0.5	2.58	2.0	
BIGO-I-1	C1	142	-2.9±0.24	-0.94±0.03	1.5±0.1	0.4	bdl	bdl	8.5±0.2	0.85	0.3	0.30
	C2		-3.3±0.1	-1.14±0.1	2.0±0.1	nd	bdl	bdl	7.6±0.2	0.76	0.9	
BIGO-I-4	C1	195	-1.3±0.08	-0.78±0.05	2.9±1.0	2.4	bdl	bdl	1.9±0.3	0.18	2.8	
	C2		-1.3±0.05	-0.69±0.04	2.6±1.4	1.6	bdl	bdl	4.5±0.1	0.43	2.2	
BIGO-II-2	C1	244	-2.3±0.1	0.18±0.03	1.7±0.14	nd	bdl	bdl	6.2±0.1	0.60	0.7	0.41
	C2		-2.5±0.3	0.63±0.15	1.3±0.17	4.6	bdl	bdl	3.3±1.1	0.32	0.6	
BIGO-II-1	C1	306	-1.5±0.06	-0.05±0.01	0.21±0.08	4.4	bdl	bdl	2.8±0.1	0.26	nd	
	C2		-1.6±0.10	nd	nd	3.8	bdl	bdl	2.6±0.02	0.23	nd	
BIGO-II-5	C1	409	-1.6±0.09	0.08±0.02	bdl	1.4	bdl	bdl	2.5±0.2	0.22	nd	0.01
	C2		-1.8±0.25	0.06±0.01	bdl	3.0	bdl	bdl	1.9±0.3	0.17	nd	
BIGO-II-3	C1	756	-0.75±0.22	bdl	bdl	2.0	bdl	-0.5	nd	nd	nd	0.05
	C2		-0.71±0.14	bdl	bdl	2.0	bdl	-1.4	5.6±0.4	0.49	nd	
BIGO-I-3	C1	989	-0.49±0.18	bdl	nd	1.2	bdl	-1.6	1.3±0.5	0.11	nd	0.01
	C2		0.23±0.10	bdl	nd	0.8	bdl	-1.1	1.1±0.1	0.09	nd	
Meteor cruise M77, 11°S, Nov/Dec 2008 [h]												
BIGO 5		85	-0.9	-2.15	4.0	1.4		bdl	8.2	0.94	2.7	
BIGO T6		259	-3.4	0.15	3.5	1.2		bdl	7.7	0.74	2.9	
BIGO 1		315	-3.2	-0.11	2.2	2.0		bdl	5.9	0.67	1.4	
BIGO 3		397	-2.8	0.05	0.7	2.0		bdl	4.0	0.45	0.5	
BIGO 2		695	-0.7	0.03	-0.05	0.7		-0.5	1.7	0.17	0	

BIGO 6		1005	-0.3	0.01	0	0.5		-1.6	2.1	0.20	0	

[a] Values marked with an asterisk are potential rates, calculated from the increase in H_2S when NO_3^- and NO_2^- became depleted inside the chamber (see text).
[b] DIC fluxes are from Dale et al. (2015).
[c] Calculated using carbon degradation rates based on DIC fluxes and the C/N ratio of organic matter at the sediment surface.
[d] DNRA = NH_4^+ flux – $NH_4^+{}_{amm}$ – N_2 fix. Values for N_2 fixation were set to zero if data were unavailable.
[e] From Gier et al. (2015). Average integrated N_2 fix rates (0 -20 cm sediment depth) were measured in sediments retrieved by a multiple corer at water depths of 70, 144, 253, 407, 770 and 1025 m.
[f] NO_2^- inside the chamber decreased to ambient values (ca. 0.3 μM) to below detection limit by the second syringe sample (ca. 4 h).
[g] NO_3^- inside the chamber decreased to ambient values (ca. 3 μM) to below detection limit by the second syringe sample (ca. 4 h).
[h] Measured DIN, NO_3^- fluxes at 11°S are from Bohlen et al. (2011) and Glock et al. (2013); remaining data are model results from Bohlen et al. (2011)

Highlights

Sulphidic event on the shelf resulted in a temporal imbalance of the benthic N cycle

Bacterial NO_x storage is a major source of oxidative power during euxinia

Peruvian shelf and upper slope sediments are strong recycling sites of fixed N

Key words

Benthic nitrogen cycle
Hypoxia
Oxygen minimum zone
Sulphur bacteria
Sulphidic event
Peru